European Radiology (2020) 30:3371–3382
https://doi.org/10.1007/s00330-020-06678-z

BREAST

Clinical relevance of total choline (tCho) quantification in suspicious lesions on multiparametric breast MRI

Claudia Sodano[1] · Paola Clauser[1] · Matthias Dietzel[2] · Panagiotis Kapetas[1] · Katja Pinker[3] · Thomas H. Helbich[1] · Alexander Gussew[4] · Pascal Andreas Baltzer[1]

Received: 6 May 2019 / Revised: 3 January 2020 / Accepted: 27 January 2020 / Published online: 17 February 2020

Abstract

Purpose To assess the additional value of quantitative tCho evaluation to diagnose malignancy and lymph node metastases in suspicious lesions on multiparametric breast MRI (mpMRI, BI-RADS 4, and BI-RADS 5).

Methods One hundred twenty-one patients that demonstrated suspicious multiparametric breast MRI lesions using DCE, T2w, and diffusion-weighted (DW) images were prospectively enrolled in this IRB-approved study. All underwent single-voxel proton MR spectroscopy (^{1}H-MRS, point-resolved spectroscopy sequence, TR 2000 ms, TE 272 ms) with and without water suppression. The total choline (tCho) amplitude was measured and normalized to millimoles/liter according to established methodology by two independent readers (R1, R2). ROC-analysis was employed to predict malignancy and lymph node status by tCho results.

Results One hundred three patients with 74 malignant and 29 benign lesions had full ^{1}H-MRS data. The area under the ROC curve (AUC) for prediction of malignancy was 0.816 (R1) and 0.809 (R2). A cutoff of 0.8 mmol/l tCho could diagnose malignancy with a sensitivity of > 95%. For prediction of lymph node metastases, tCho measurements achieved an AUC of 0.760 (R1) and 0.788 (R2). At tCho levels < 2.4 mmol/l, no metastatic lymph nodes were found.

Conclusion Quantitative tCho evaluation from ^{1}H-MRS allowed diagnose malignancy and lymph node status in breast lesions suspicious on multiparametric breast MRI. tCho therefore demonstrated the potential to downgrade suspicious mpMRI lesions and stratify the risk of lymph node metastases for improved patient management.

Key Points

- *Quantitative tCho evaluation can distinguish benign from malignant breast lesions suspicious after multiparametric MRI assessment.*
- *Quantitative tCho levels are associated with lymph node status in breast cancer.*
- *Quantitative tCho levels are higher in hormonal receptor positive compared to hormonal receptor negative lesions.*

Keywords Magnetic resonance spectroscopy · Magnetic resonance imaging · Breast neoplasms · Prognosis · Sensitivity and specificity

Claudia Sodano and Paola Clauser contributed equally to this work.

Electronic supplementary material The online version of this article (https://doi.org/10.1007/s00330-020-06678-z) contains supplementary material, which is available to authorized users.

✉ Pascal Andreas Baltzer
pascal.baltzer@meduniwien.ac.at

[1] Department of Biomedical Imaging and Image-guided Therapy, Division of Molecular and Gender, Imaging, Medical University of Vienna, Waehringer-Guertel 18-20, A-1090 Vienna, Austria

[2] Institute of Radiology, Universitätsklinikum Erlangen, Maximiliansplatz 1, 91054 Erlangen, Germany

[3] Department of Radiology, Breast Imaging Service, Memorial Sloan Kettering Cancer Center, 300 E 66th Street, New York, NY 10065, USA

[4] Universitätsklinik und Poliklinik für Radiologie, Ernst-Grube-Str. 40, D-06120 Halle (Saale), Germany

Abbreviations

^{1}H-MRS, MRS	Proton MR spectroscopy
ADC	Apparent diffusion coefficient
AUC	Area under the curve
BI-RADS	Breast imaging–reporting and data system
DCE	Dynamic contrast enhanced
DWI	Diffusion-weighted imaging
FLASH	Fast low angle shot
GRAPPA	GeneRalized Autocalibrating Partial Parallel Acquisition
IRB	Institutional Review Board
MRI, mpMRI	Magnetic resonance imaging, multiparametric MRI
PRESS	Point Resolved Spectroscopy Sequence
ROC	Receiver operating characteristics
tCho	Total choline
TE	Echo time
TR	Repetition time
TSE	Turbo spin echo

Introduction

Breast cancer is a major burden on the female population and subsequently for the socioeconomic system. Consequently, most industrialized nations have introduced nation-wide mammography screening programs that are supported by the majority of specialist societies [1]. Screening with mammography and additional evaluations with ultrasound and MRI add in cancer diagnosis and assessment of disease [2–4].

Currently, breast cancer is treated by a combination of surgery, pharmaceutical therapy, and radiation therapy tailored to the individual patient based on risk factors including cancer type, lymph node metastases, and menopausal status [5]. To select the best treatment option, breast cancer needs to be diagnosed and accurately characterized. Although breast cancer type can be determined using image-guided biopsies, biopsies only provide information on the biopsied part of the lesion which is subject to selection bias, potentially leading to inaccurate diagnoses. It has been demonstrated that imaging characteristics, in particular those derived from breast MRI, can help to identify prognostically relevant information [6–11]. Lymph node status is more challenging to assess: metastatic lymph nodes might be present even if suspicious imaging characteristics are absent [12–14], and in some cases of lymph nodes with uncertain morphology it might be difficult to perform a biopsy and confirm or exclude metastasis. Thus, there is a need for more accurate and non-invasive methods to determine lymph nodes status before treatment.

Proton MR spectroscopy (^{1}H-MRS) allows the assessment of total choline (tCho), a compound resonance that is connected to multiple enzymatic changes involved in oncogenesis, tumor progression, and metastasis [15]. ^{1}H-MRS has therefore been proposed as an additional tool to improve lesion characterization, but its use has been restricted due to the technical difficulties related to data acquisition and interpretation, yielding heterogeneous results [16]. Nevertheless, ^{1}H-MRS is able to give information on a molecular level without the use of contrast agents, and its feasibility is highly improved owing to the improved performance of magnets and coils. Accurate breast cancer diagnosis including lymph node status is pivotal in determining treatment and currently requires biopsies and open surgery. We hypothesize that the additional molecular information provided by ^{1}H-MRS can be used to facilitate breast lesion workup by potentially avoiding invasive diagnostic procedures to diagnose breast cancer and lymph node metastases.

The aim of this study was to evaluate the additional value of quantitative tCho evaluation to diagnose malignancy, breast cancer type, and lymph node status in suspicious lesions on multiparametric breast MRI (mpMRI, BI-RADS 4, and BI-RADS 5).

Methods

Study design, participants, and reference standard

This prospective, IRB-approved single-center cross-sectional study was performed at the university hospital of Jena, Germany, a certified tertiary care academic breast center. The study aimed to evaluate the additional value of tCho measurements from ^{1}H-MRS to diagnose malignancy, breast cancer type, and lymph node status in MRI BI-RADS 4 and BI-RADS 5 lesions. A summary of the study design is given in Supplementary figure 1. Eligible were consecutive patients undergoing breast MRI for further workup of equivocal and suspicious conventional imaging (digital mammography, MG; ultrasound, US) findings (BI-RADS 0, BI-RADS 4, and BI-RADS 5). To be further eligible for this study, they had to present with a contrast-enhancing lesion of at least 8 mm in size on the MRI scan that was rated as suspicious (MRI BI-RADS 4 and BI-RADS 5) according to pre-defined criteria: non-circumscribed or spiculated margins, type II or III curve, non-circumscribed, non-hyperintense T2w correlate, and intermediate to low apparent diffusion coefficient (ADC) values $< 1.5\ 10^{-3}$ mm^2/s were considered suspicious, the combined appearance of several of these criteria as highly suspicious. This initial assessment was done by one of two breast MRI experts (W.A.K., P.A.B.) while the patient was placed in the scanner and MR spectroscopy was performed in eligible patients in the same breast MRI examination. Exclusion criterion was missing informed consent. Note that ineligibility for contrast-enhanced MRI was not counted as an exclusion criterion as patients were recruited before the MRI examination at the day of their visit while claustrophobia,

presence of allergies, and metallic implants were excluded when scheduling the MRI appointment. Patients were excluded from the final analysis in case of termination of the examination before completion, incomplete imaging data, or non-interpretable imaging data due to artifacts (e.g., caused by motion).

Histopathologic workup of the patients served as the reference standard and was always performed after the breast MRI scan. Spectroscopy results were not used to guide patient management decisions. Biopsies were performed either US-guided by 14-gauge core needle biopsy in case of US visibility or MRI-guided 9G console-mounted vacuum-assisted biopsy in case the lesion was not visible on conventional imaging. All malignant lesions underwent surgery. If there was a discordance between biopsy and surgery, the latter was used as reference standard. However, if the patient was treated by neoadjuvant therapy, the histopathological result from the biopsy was used as reference standard. Benign results were checked for consistency within weekly interdisciplinary meetings and re-biopsied or operated on when deemed necessary (inconclusive results, e.g., B1 or unspecific B2 in case of circumscribed lesions). Lesions with uncertain malignant potential (B3) upon histopathology were surgically removed [17]. Benign B2 findings deemed consistent with histopathology were followed up by the imaging test best suited to visualize the lesion (either MG, US, or MRI) over 24 months as has been done in prior studies (e.g., listed in [18]). At the time of the study, sentinel lymph node biopsy (SNLB) was performed in all surgeries of malignant lesions. In case of positive SNLB, axillary lymph node dissection was performed. For the lymph node analysis in this study, only patients that underwent axillary surgery without prior neoadjuvant therapy were used. The study design is summarized in a flowchart (Supplementary Fig. 1).

MR imaging and proton MR spectroscopy

All imaging was performed on a 1.5-T scanner (Siemens Magnetom Sonata, Siemens Healthineers) using the dedicated vendor-supplied 4-channel double breast coil. The standardized protocol was in accordance with international recommendations and employed an axial 2D T2-w turbo spin echo (TSE, TR 8900 ms, TE_{eff} 207 ms, field of view 340 mm, matrix 512 mm, slice thickness 3 mm) and a dynamic T1-weighted spoiled gradient echo sequence (fast low angle shot, FLASH, GRAPPA factor 2, TR 113 ms, TE 5 ms, FOV 340 mm, matrix 384, slice thickness 3 mm). Afterwards, 0.1 mmol/l body weight of gadopentetate dimeglumine (Gd-DTPA, Magnevist) was administered intravenously as a rapid bolus (3 ml/s), performed by an automatic injector (Spectris, Medrad), followed by 20 ml saline solution. The dynamic scan had a temporal resolution of 1 min and was repeated 8 times. An injection delay of 30 s between scans 1 (precontrast) and 2 (first postcontrast acquisition) was applied. In addition, a diffusion-weighted Echo Planar Imaging (EPI) sequence (GRAPPA factor 2, TR 3500, TEeff 80, echo distance 0.95 ms, six averages, three b-values: 0, 750, 1000 s/mm^2, spectral fat saturation, in plane resolution 1.8 × 1.8 mm, slice thickness 6 mm) was acquired. Apparent diffusion coefficient (ADC) maps were calculated in-line by the scanner software.

Proton MR spectroscopy (^{1}H-MRS, vendor-supplied standard single-voxel point-resolved spectroscopy sequence PRESS, TR 2000 ms, TE 272 ms, vector size 1024, weak water suppression with a bandwidth of 35 Hz, 128 averaged acquisitions with an acquisition time of 4:16 min) was acquired after automatic and manual first- and second-order shim gradient adjustments. The full width at half maximum was usually below 25 Hz. An additional scan without water suppression using 32 averages and the same adjustments was subsequently acquired as an internal reference. Including planning and shimming, spectroscopy was performed within 8–10 min. All spectra acquisitions were performed by an experienced breast radiologist trained in MR spectroscopy and acquisition (referred to as investigator, > 10 years of experience, P.A.B.) and supervised by two dedicated spectroscopists (> 25 and > 10 years of experience, A.G., R.Z.).

Data analysis

All acquired spectra were technically reviewed by the investigator after acquisition using the vendor-supplied software and then exported as raw data (.rda file) for further analysis. Consecutive analysis by two independent readers (both radiologists with > 2 years of training, supervised by the investigator) was done using v 4.0 of the free java Magnetic Resonance User Interface (jMRUI) software (www.jmrui.eu). The readers knew the study design but were not aware of any specific patient-related data. FID data were zero filled to 2048 data points and a Gaussian apodization of 5 Hz was applied. Fourier transformation and manual phase correction followed. The spectra were referenced using the water and methylene peaks as reference (4.74 and 1.33 ppm). Quantification was done by the AMARES algorithm [19] using prior knowledge on peak position (soft constraints ± 0.15 ppm) and tCho peak amplitude (soft constraints 0–200 arbitrary units). The fitting result was compared to the original spectrum by subtraction and was considered acceptable if systematic baseline deviations > 1.5-fold higher the baseline noise were absent. In case of an insufficient quantitation of tCho at 3.23 ppm, soft constraints for peak amplitude were adapted based on overall noise level and visual inspection of visible tCho peaks. The fitting procedure was repeated until the subtracted peak yielded a zero baseline as defined above. Absolute tCho

concentrations were quantified in mmol/l by using the following equation:

$$C_{\mathrm{Cho}} = \frac{I_{\mathrm{cho}}}{I_{\mathrm{wat}}} \cdot \frac{N^{H}_{\mathrm{wat}}}{N^{H}_{\mathrm{cho}}} \cdot \frac{R_{\mathrm{wat}}}{R_{\mathrm{Cho}}} \cdot C_{\mathrm{wat}}$$

$$R_x = \mathrm{e}^{-\frac{\mathrm{TE}}{T^x_2}} \cdot \left(1 - \mathrm{e}^{-\frac{\mathrm{TR}}{T^x_1}}\right)$$

While the water concentration was approximated to 55,600 mmol/l, the hydrogen quantities in water and choline molecules were set to 2 and 9, respectively. Finally, T_1 and T_2 relaxation times of water and choline were adapted from a review article of Haddadin et al ($T_1^{\mathrm{wat}} = 0.441$ s; $T_1^{\mathrm{Cho}} = 1.513$ s; $T_2^{\mathrm{wat}} = 0.075$ s; $T_2^{\mathrm{Cho}} = 0.269$ s) [20, 21].

In addition, lesion size was measured volumetrically by assessing lesion dimensions in all three plains on early DCE images acquired 2 min after CM injection. The lesion volume was calculated in milliliters by multiplying the lesion size in all three plains in centimeters with 0.52 and expressed in milliliters.

Statistical analysis

Continuous variables are presented by median, interquartile range, and range. Quantitative tCho values were calculated according to the formula above and compared between lesion subgroups using non-parametric statistics (Mann-Whitney *U* test in case of two independent samples, Kruskal-Wallis test in case of > 2 independent samples). Bland-Altman statistics were performed to calculate mean differences and limits of agreement between both tCho measurements of R1 and R2.

The area under the receiver operating characteristics (ROC) curve (AUC) was used as a measure of diagnostic performance for tCho measurements. Two independent sets of

Table 1 Lesion characteristics

Lesions characteristics			tCho (R1, mmol/kg)[#]	tCho (R2, mmol/kg)[#]	*p* value
Malignant lesion histological subtypes		*n* = 74	3.22 (2.07, 7.17; 0.23–15.89)	3.29 (1.83, 7.28; 0.22–16.00)	
	Invasive ductal carcinoma NST	57	2.82 (2.01, 7.32; 0.23–15.89)	2.95 (1.78, 7.32; 0.22–16.00)	0.346 (R1), 0.301 (R2)
	Invasive lobular carcinoma	12	4.36 (2.66, 7.51; 1.04–11.19)	4.20 (2.94, 8.45; 1.41–11.01)	
	Ductal carcinoma in situ	2	3.57 (3.03, 4.12; 3.03–4.12)	3.29 (3.26, 3.32; 3.26–3.32)	
	Other[§]	3	1.79 (0.99, 2.87; 0.73–3.23)	1.96 (1.03, 2.68; 0.72–2.93)	
Malignant lesion grading		*n* = 74			
	G1	5	1.65 (1.07, 4.79; 0.62–7.79)	1.74 (1.01, 5.50; 0.49–9.05)	0.200 (R1), 0.264 (R2)
	G2	26	3.57 (2.65, 7.41; 0.23–15.89)	3.70 (2.67, 7.62; 0.22–16.00)	
	G3	43	3.11 (1.82, 6.30; 0.54–13.22)	3.10 (1.75, 6.33; 0.83–13.17)	
Malignant lesion receptor status		*n* = 73*			
	HR+, her2neu−	38	4.42 (2.62, 7.94; 0.23–15.89)	4.25 (2.66, 4.27; 0.22–16.0)	0.051 (R1), 0.056 (R2)[x]
	HR+, her2neu+	15	3.20 (2.67, 4.09; 1.70–7.32)	2.95 (2.66, 4.27; 1.41–8.73)	
	HR−, her2neu+	6	2.41 (1.58, 2.48; 1.33–4.00)	2.37 (1.51, 2.42; 1.29–3.71)	
	HR−, her2neu−	14	1.95 (1.69, 6.47; 0.84–11.19)	1.81 (1.70, 6.74; 0.83–11.01)	
Lymph node status		*n* = 63*			
	LN+	17	7.17 (3.78, 8.43; 2.48–13.22)	8.19 (3.81, 8.81; 2.42–13.17)	0.002 (R1), < 0.001 (R2)
	LN−	46	2.79 (1.75, 2.66; 0.23–15.89)	2.86 (1.71, 4.92; 0.22–16.00)	
	Benign lesions	*n* = 29	0.93 (0.27, 2.55; 0.00–6.00)	1.13 (0.27, 2.57; 0.00–6.06)	
	Epithelial proliferations	15	1.07 (0.13, 2.94; 0.00–6.00)	1.10 (0.11, 2.89; 0.00–6.06)	0.919 (R1), 0.872 (R2)
	Fibroadenoma	8	1.13 (0.09, 3.37; 0.00–4.78)	1.13 (0.09, 3.59; 0.00–5.03)	
	Solid B3[$]	3	1.93 (0.30, 2.16; 0.30–2.16)	2.11 (0.41, 2.22; 0.41–2.22)	
	Inflammation	3	0.73 (0.26, 0.93; 0.26–0.93)	0.84 (0.25, 1.13; 0.25–1.13)	

* in 11 patients, no reliable reference standard for axillary lymph node status was available due to neoadjuvant treatment before surgery and in one patient no receptor status was available in a DCIS; [#] given as: median (interquartile range Q25, Q75, range); [§] one invasive papillary, mucinous, and tubular carcinoma, respectively; [$] two papilloma, one phyllodes; [x] HR+ breast cancers differed significantly from all others ($p = 0.018$ (R1) and $p = 0.020$ (R2), respectively

ROC analyses were performed for R1 and R2, respectively: diagnosis of benign vs malignant and diagnosis of lymph node status (negative vs positive) in malignant lesions. The null hypothesis was defined as AUC = 0.5. To determine exploratory tCho cutoff values, we followed the approach of identifying an exploratory "rule-out" criterion for malignancy [22, 23]. Such a criterion was considered present if the corresponding tCho cutoff yielded a sensitivity of ≥ 95% in both readers. As all lesions in this study were considered suspicious by mpMRI (T2w; diffusion-weighted imaging, DWI; dynamic contrast enhanced, DCE), the specificity value at this cutoff indicates the rate of benign lesions that may not have required biopsy if the tCho value was below this exploratory threshold. *P* values of < 0.05 were considered statistically significant.

All statistical analyses were performed using Medcalc 18.10.2 software.

Results

General

One hundred twenty-one patients were examined with the study protocol. Eighteen of these (14.9%) had to be excluded due to technically insufficient spectra (bulk motion during acquisition and wrongly applied water suppression in the reference scan being the most common reasons). Finally, 103 patients had full diagnostic and reference data and were eligible for further analysis (median age 55 years, range 23–83 years) with 103 lesions (74 malignant, 29 benign, lymph node status was positive in 17 and negative in 46 breast cancers; in 11 patients no reliable reference standard for axillary lymph node status was available due to neoadjuvant therapy before surgery. See Table 1 for histological details and Supplementary figure 1 for the patient selection flowchart). Lesion volumes ranged from 0.45 to 274.6 ml with a median volume of 3.98 ml. No significant differences were found between median volumes of benign (3.59 ml, range 0.47–61.92 ml) and malignant (4.06, range 0.45–274.6 ml) lesions ($p = 0.401$, Mann-Whitney *U* test). Spectroscopy voxel sizes ranged between 1.73 and 27 ml with a median volume of 5.83 ml.

tCho levels in benign and malignant lesions

tCho levels were significantly higher in malignant compared to benign lesions ($p < 0.001$ for both R1 and R2, respectively, see Table 1 and supplementary figure 2). While highest tCho levels were observed in ILC (see Table 1), these differences compared to other cancer subgroups did not prove statistically significant ($p = 0.346$, R1; $p = 0.301$, R2). Lower tCho was observed in G1 as compared to G2 and G3 cancers (Table 1), again without demonstrating statistical significance ($p = 0.200$, R1; $p = 0.264$, R2).

Full receptor status was available in 73 of 74 malignant lesions (Table 1). Figure 1 shows tCho levels stratified by breast cancer receptor status. The tCho levels in hormonal receptor positive breast cancers were significantly higher than those in hormonal receptor negative lesions ($p = 0.018$, R1; $p = 0.020$, R2). No further subgroup differences between breast cancer subgroups as distinguished by receptor status were found ($p = 0.051$, R1 and $p = 0.056$, R2).

In 63 cancer patients with available lymph node status (11 without reference standard after neoadjuvant breast cancer treatment), tCho levels were significantly higher in those with

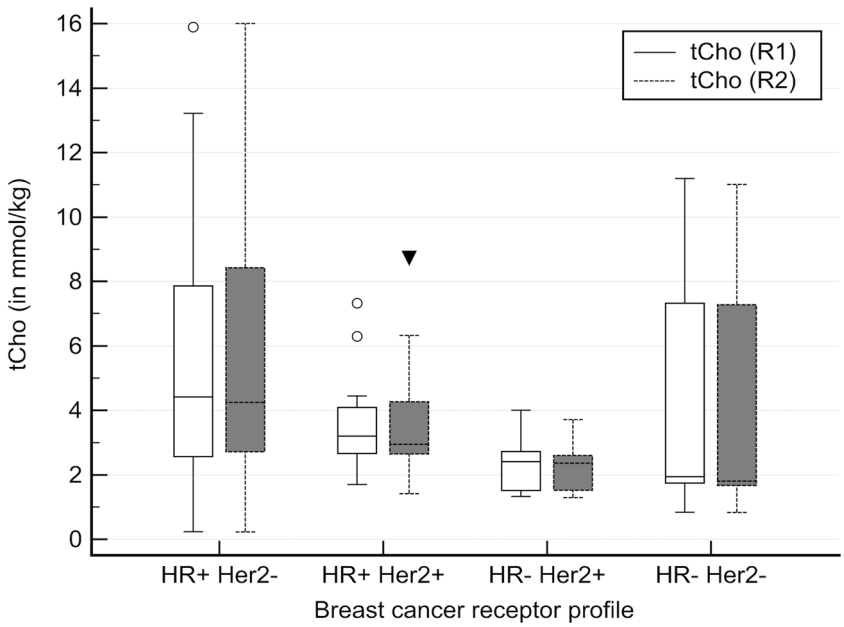

Fig. 1 Boxplots of tCho results stratified by breast cancer receptor status (HR: hormonal receptors, Her2+: her2neu receptor status, + indicating positivity, − negativity). The observed tCho levels were significantly higher in hormonal receptor positive breast cancers ($p = 0.018$, R1; $p = 0.020$, R2)

positive as compared to negative lymph nodes ($p = 0.002$, R1; $p < 0.001$, R2, Table 1).

In benign lesions, no significant subgroup differences were found ($p = 0.919$, R1; $p = 0.872$, R2; see Table 1).

Reproducibility of tCho quantification on acquired spectroscopy data

Figure 2 demonstrates Bland-Altman plots for differences and limits of agreement between R1 and R2 as absolute (Fig. 2a) and percentage (Fig. 2b). The absolute mean difference between R1 and R2 was − 0.06 mmol/l, the limits of agreement ranging between − 0.76 and 0.65 mmol/l. The relative mean difference between R1 and R2 was − 1.2%, the limits of agreement ranging between − 25.4 and 23.0%.

tCho to distinguish benign from malignant breast lesions

Figure 3 and Table 2 display the results of the ROC analysis. tCho showed a good area under the curve to distinguish benign from malignant lesions as measured by the AUC (0.816 (R1) and 0.809 (R2), $p < 0.0001$ for R1 and R2, respectively). The ROC curve analysis revealed that if tCho was

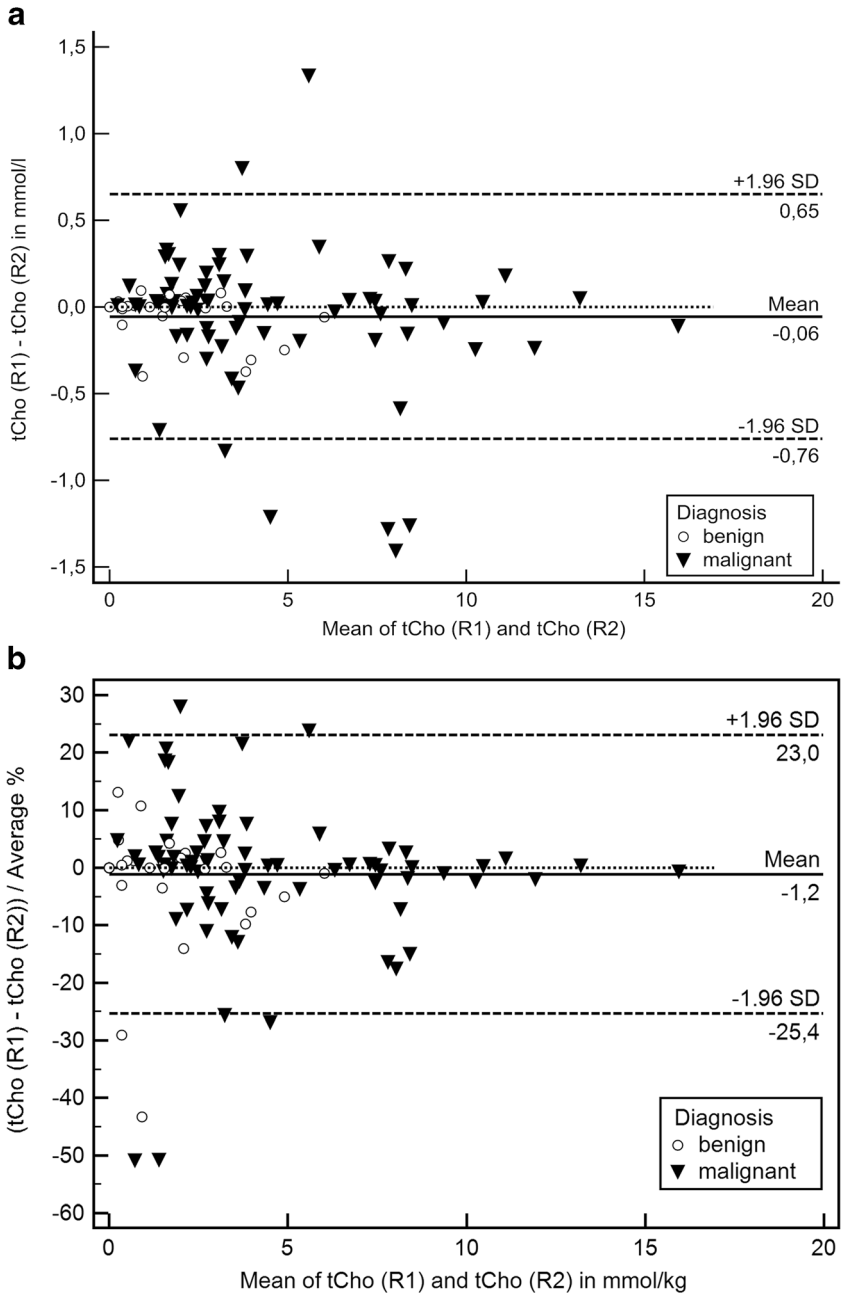

Fig. 2 Bland-Altman plots of tCho differences between R1 and R2. **a** Absolute differences; **b** relative differences

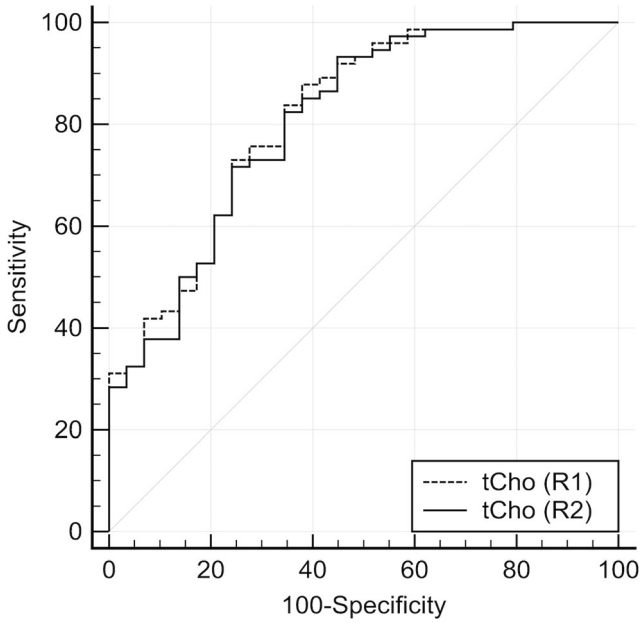

Fig. 3 Receiver operating characteristic (ROC) curves estimating diagnostic performance of tCho to distinguish benign from malignant breast lesions ($n = 103$). Lesion volume serves as a reference and did not predict the presence of cancer ($p > 0.05$)

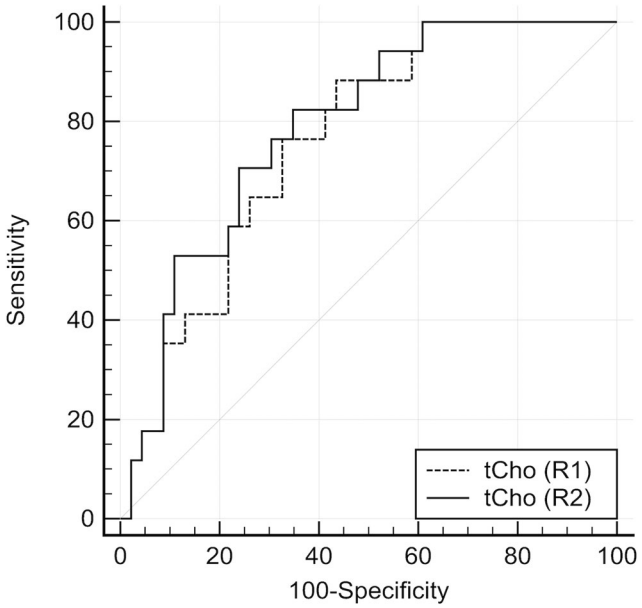

Fig. 4 Receiver operating characteristics (ROC) curves estimating diagnostic performance of tCho to predict the presence or absence of metastatic lymph nodes ($n = 63$). Lesion volume serves as a reference and did not predict the presence of lymph node metastases ($p > 0.05$)

≤ 0.8 mmol/l, sensitivity for detection of breast cancer exceeded 95% for both readers (also see supplementary figure 2). Applying this threshold, could have potentially avoided $n = 14/29$ (48.3%, R1) or $n = 13/29$ (44.8%, R2) unnecessary biopsies in the investigated cohort while yielding $n = 3/74$ (4.1%, R1) or $n = 2/74$ (2.7%, R2) false negative diagnoses (two T1b hormonal receptor positive NST G2, one T1c hormonal receptor positive invasive tubular carcinoma G1).

tCho to predict positive lymph node metastasis

Figure 4 and Table 3 summarize ROC analysis results. Primary lesion tCho could significantly predict lymph node status with an AUC of 0.760 (R1, $p < 0.0001$) and 0.788 (R2, $p < 0.0001$). Below a tCho of 2.4 mmol/l, no metastatic lymph nodes where observed, thus achieving a sensitivity of 100% in both readers (also see supplementary figure 3). This condition applied to 39.1% (18/46) of all non-metastatic cancers in both R1 and R2. Details are given in Table 3. Clinical example cases are shown in Fig. 5 and Fig. 6.

Discussion

Quantitative tCho evaluation from ^{1}H-MRS allowed to diagnose malignancy and lymph node status in breast lesions that were considered suspicious with multiparametric breast MRI assessment using DCE, T2w and diffusion-weighted (DW) images. Specifically, low tCho concentrations associated with a low risk of breast cancer and lymph node metastasis. If confirmed by prospective studies, these findings would be of high clinical relevance as positive findings on MRI require invasive workup in order to avoid unnecessary surgery [24]. Further, the availability of MRI-guided interventions is limited [25], stressing the need for non-invasive tools to avoid unnecessary biopsies. While lymph node status is one of the most important predictors of breast cancer outcome, surgical management is increasingly conservative, avoiding axillary lymph node dissection in case of limited disease [26–28]. Again, a non-invasive tool to accurately assess the risk of present lymph node metastases could facilitate the clinical workup of breast cancer patients.

Table 2 Diagnostic performance estimates and cutoff values for tCho to distinguish benign ($n = 29$) from malignant ($n = 74$) breast lesions

Parameter	AUC	*p* value	tCho cutoff in mmol/l	Sensitivity (95% CI) in %	Specificity (95% CI) in %
tCho (R1)	0.816	< 0.0001	0.8	96.0 (88.6–99.2)	48.3 (29.4–67.5)
tCho (R2)	0.809	< 0.0001	0.8	97.3 (90.6–99.7)	44.8 (26.4–64.3)

Table 3 Diagnostic performance estimates and cutoff values for tCho to predict the presence ($n = 17$) or absence ($n = 43$) of metastatic lymph nodes

Parameter	AUC	*p* value	tCho cutoff mmol/l	Sensitivity (95% CI) in %	Specificity (95% CI) in %
tCho (R1)	0.760	< 0.0001	2.4	100 (80.5–100)	39.1 (25.1–54.6)
tCho (R2)	0.788	< 0.0001	2.4	100 (80.5–100)	39.1 (25.1–54.6)

We were not the first group to investigate quantitative tCho measurements using an internal reference to distinguish benign from malignant breast lesions (see Table 4). Prior reports differed regarding their results, either reporting very high sensitivity and specificity [29, 30], very high specificity but moderate sensitivity [31], and only one group reported moderate sensitivity and specificity [32]. These different results can both be explained by the application of different thresholds and different patient and lesion groups. All groups examined lesions above 0.7 cm in size [29–32] and two reports pre-defined a minimum size of the investigated lesions and focused on mass lesions only [29, 31]. Our specificity is seemingly lower than previously reported (see Table 4). This is due to the different study design: opposed to prior reports, our study investigated whether MR spectroscopy can further improve diagnosis of suspicious mpMRI findings. The specificity values at the tCho threshold associated with a high sensitivity can thus be directly translated into the rate of avoidable biopsies of benign lesions [23]. Our results are possibly best compared to those of Dorrius et al, who investigated a comparable setting. In their study, the authors used ^{1}H-MRS as an additional test to rule out cancer in a problem-solving setting using a three-dimensional spatially resolved spectroscopy technique [33]. We did not in detail investigate the effects of single techniques on diagnostic outcomes as reported by Pinker et al [34]. This was due to the fact that the study rationale was using MR spectroscopy only in case of suspicious multiparametric MRI using T2w, DWI, and DCE sequences. While several formal approaches of integrating these data into a diagnosis have been reported [35–38], our study protocol relied on the classical empirical approach of assigning BI-RADS categories. Our study design, however, allows to estimate the potential downgrade rates of benign breast lesions appearing suspicious upon triparametric (T2w, DWI, DCE) MRI as > 40%.

We observed higher tCho levels in hormonal receptor–positive breast cancers. This seems to be in line with reports on choline kinase deregulation promoting estrogen receptor-driven proliferation [39]. Similar findings have been reported by Sah et al [32]. While the significance of this finding, e.g., on the general applicability of the exploratory tCho thresholds provided within this study cannot be estimated due to the limited sample size of our study (all FN findings were hormonal receptor positive), implications arise regarding the potential prediction of antihormonal treatment response. The tCho concentrations in our study fall within the range reported in prior studies (see Table 4). Note, however, that though using water as an internal reference addresses several normalization aspects such as voxel size and coil sensitivity differences, the method applied here and in the referenced papers relies on fixed assumptions regarding the real water concentration in tissue as well as the relaxation times of water and tCho in vivo [20]. Individual variations of these parameters, in

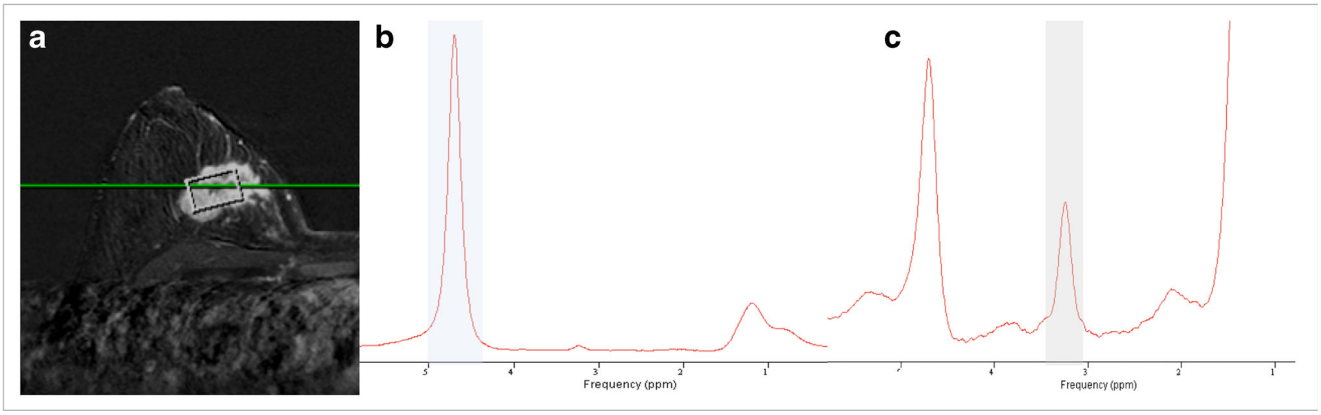

Fig. 5 Thirty-four-year-old woman presenting with an enhancing suspicious mass in the early contrast enhanced subtraction image (**a**). **b** presents the water resonance peak at 4.74 ppm in the unsuppressed water reference spectrum (blue bar), weaker resonance peaks can be depicted at 3.23 (corresponding to total Choline tCho) and 1.3 and 0.9 ppm (methylene and methyl groups from lipids). The magnified water suppressed spectrum reveals the distinct tCho resonance peak at 3.23 ppm (gray bar). Using water as an internal reference, tCho was calculated as 13 mmol/l. Histopathology revealed an invasive ductal cancer NST G3 with ipsilateral lymph node metastases

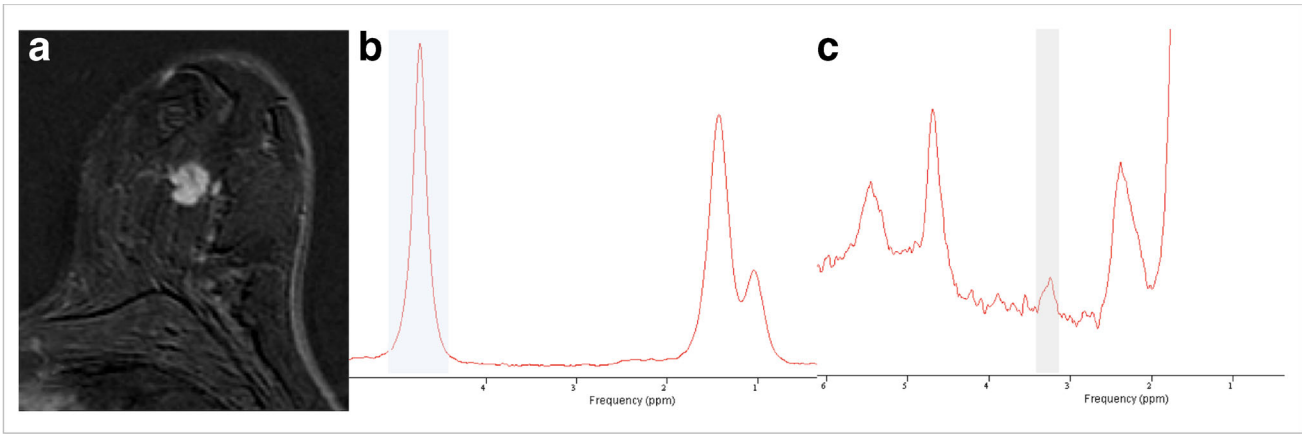

Fig. 6 Forty-six-year-old woman presenting with an enhancing suspicious mass in the early contrast enhanced subtraction image (**a**). **b** presents the water resonance peak at 4.74 ppm in the unsuppressed water reference spectrum (blue bar). The magnified water suppressed spectrum reveals a weak tCho resonance peak at 3.23 ppm (gray bar). Using water as an internal reference, tCho was calculated as 1.9 mmol/l. Histopathology revealed an invasive ductal cancer NST G2 and negative lymph nodes

particular tissue water concentration that might vary due to patient hydration, age, treatment and hormonal status, likely explain differences regarding tCho concentrations reported in the individual studies. We demonstrated a good reproducibility of tCho quantitation using the AMARES method. Though important in the field of imaging biomarker research, this aspect has only been investigated in other techniques such as breast DWI [40]. Due to the clinical study design, we did not analyze the repeatability of ^{1}H-MRS data acquisition and inter-scanner variability. In this context, individual measurements of tCho and water relaxation times might be desirable in order to assess their potential impact and weigh it against the additional measurement time required. Therefore, all quantitative thresholds must be regarded as exploratory only until independently validated. Another issue is the potential interaction of tCho with contrast media that is further outlined below.

Our study results further indicate that the primary breast cancer tCho levels are predictive for lymph node metastases. Specifically, a low tCho concentration indicated the absence of lymph node metastases in a substantial proportion of our breast cancer cases. If prospectively validated, sentinel node biopsies (SNB) could be potentially avoided in patients classified as being at low risk for lymph node metastasis. While anecdotal and encouraging evidence exists on direct ^{1}H-MRS in axillary lymph nodes [41], a direct measurement would require visibly enlarged lymph nodes and a time-consuming additive measurement. Indirect axillography based on an imaging phenotype of the index breast cancer has been shown by Dietzel et al in a radiomic approach using artificial neural networks on semantic lesion features [42]. Whether ^{1}H-MRS data can contribute to prognostic breast cancer models or adds to morphological lymph node assessment remains to be investigated.

Our analysis is limited regarding several aspects: first, our spectroscopy technique is not spatially resolved. Though prior reports have reported encouraging results on spatially resolved ^{1}H-MRS, quantification is still not established and difficult to achieve within a non-research setting. In addition, while theoretically of benefit, a spatially resolved spectroscopy still can only cover a region of interest and not two breasts. In the investigated application of ^{1}H-MRS, that is the downgrading of lesions suspicious on conventional MRI assessment, it is of limited relevance to yield spatially resolved images as the area

Table 4 Summary of prior reports on tCho quantification based on single-voxel acquisitions and comparison with the results reported in this paper

First author/year	Field strength	Cases	Cancer prevalence (%)	Sensitivity (%)	Specificity (%)	tCho* range
Thakur/2011 [1]	1.5 T	88	64.8	96.5	93.5	0–47.1
Baek/2012 [2]	1.5 T	112	88.4	65.7	92.3	0.9–10
Sah/2012 [3]	1.5 T	189	79.9	76.2	76.3	$^{+}$0.58/1.6/4.2–5.4
Suppiah/2012 [4]	1.5 T	57	73.7	95.2	93.3	0.1–6.9
This study/2018	1.5 T	103	71.8	95.9	48.3$^{\#}$	0–16

* in mmol/l; $^{+}$ [1–4] no range given. Values indicate mean values for healthy tissue, benign and malignant lesions. Malignant lesions were reported in subgroups. $^{\#}$ This study investigated only lesions classified as BI-RADS 4 or BI-RADS 5 after full triparametric (T2w, DWI, DCE) breast MRI assessment. Thus, the reported specificity does only apply to tCho quantification as investigated in this specific situation

of interest is directly investigated. In this respect, our study is unique as we decided to use ^{1}H-MRS on the spot, that is while the patient was still in the scanner. We are well aware that in many institutions MRI scans are acquired and interpreted at different time points and even different physical locations. While our approach may thus be difficult to employ in some institutions, the results do still apply: ^{1}H-MRS has an additional diagnostic value in mpMRI of the breast and provides additional, prognostically relevant information on lymph node status. The PRESS sequence used had a long echo time. While shorter echo times may increase the tCho signal, TE is considered in the quantitation procedure. Besides, a meta-analysis reported no influence of TE on diagnostic performance of Cho assessment by ^{1}H-MRS [16]. One potential drawback is the need for IV contrast. Gd-based contrast media show an interaction with the tCho signal in vivo [43], an effect that has been reported as being more pronounced in ionic contrast media and thus must be considered when comparing different study results [44]. Acquisition time is a further limitation of the used approach. Though aiming at screening, there is a trend to reduce magnet times in breast MRI and an additional test must prove its value also regarding magnet time efficiency [45]. Modern 3-T systems in combination with multichannel coils could substantially reduce acquisition times due to SNR gain that is more than fourfold [46] while a reduction of averages by 50% would only reduce the SNR by square root of 2. Consequently, the acquisition times reported here could potentially be reduced to 3 min or less while yielding the same SNR.

In conclusion, quantitative tCho evaluation from ^{1}H-MRS allowed to diagnose malignancy and lymph node status in breast lesions that are considered suspicious with multiparametric breast MRI assessment using DCE, T2w, and diffusion-weighted (DW) images. tCho demonstrated the potential to improve diagnosis of malignancy in breast MRI lesions suspicious on mpMRI and stratify the risk of lymph node metastases with the aim of improved patient management.

Funding Information Open access funding provided by Medical University of Vienna. This study has received funding by the Austrian National Bank Jubiläumsfonds project number 17186.

Compliance with ethical standards

Guarantor The scientific guarantor of this publication is Pascal A.T. Baltzer.

Conflict of interest The authors of this manuscript declare no relationships with any companies whose products or services may be related to the subject matter of the article.

Statistics and biometry One of the authors has significant statistical expertise.

Informed consent Written informed consent was obtained from all subjects (patients) in this study.

Ethical approval Institutional Review Board approval was obtained.

Methodology
- Prospective
- Cross-sectional study
- Performed at one institution

References

1. Sardanelli F, Aase HS, Álvarez M et al (2017) Position paper on screening for breast cancer by the European Society of Breast Imaging (EUSOBI) and 30 national breast radiology bodies from Austria, Belgium, Bosnia and Herzegovina, Bulgaria, Croatia, Czech Republic, Denmark, Estonia, Finland, France, Germany, Greece, Hungary, Iceland, Ireland, Italy, Israel, Lithuania, Moldova, The Netherlands, Norway, Poland, Portugal, Romania, Serbia, Slovakia, Spain, Sweden, Switzerland and Turkey. Eur Radiol 27:2737–2743. https://doi.org/10.1007/s00330-016-4612-z
2. Mann RM, Kuhl CK, Kinkel K, Boetes C (2008) Breast MRI: guidelines from the European Society of Breast Imaging. Eur Radiol 18:1307–1318. https://doi.org/10.1007/s00330-008-0863-7
3. Sardanelli F, Boetes C, Borisch B, et al (2010) Magnetic resonance imaging of the breast: recommendations from the EUSOMA working group. Eur J Cancer Oxf Engl 1990 46:1296–1316. https://doi.org/10.1016/j.ejca.2010.02.015
4. American College of Radiology (ACR) (2014) ACR practice parameter for the performance of contrast-enhanced magnetic resonance imaging (MRI) of the breast. Available via https://www.acr.org/-/media/ACR/Files/Practice-Parameters/mr-contrast-breast.pdf
5. Senkus E, Kyriakides S, Ohno S et al (2015) Primary breast cancer: ESMO clinical practice guidelines for diagnosis, treatment and follow-up. Ann Oncol 26(Suppl 5):v8–v30. https://doi.org/10.1093/annonc/mdv298
6. Kim MY, Choi N (2013) Mammographic and ultrasonographic features of triple-negative breast cancer: a comparison with other breast cancer subtypes. Acta Radiol 54:889–894. https://doi.org/10.1177/0284185113488580
7. Costantini M, Belli P, Distefano D et al (2012) Magnetic resonance imaging features in triple-negative breast cancer: comparison with luminal and HER2-overexpressing tumors. Clin Breast Cancer 12:331–339. https://doi.org/10.1016/j.clbc.2012.07.002
8. Youk JH, Son EJ, Chung J, Kim JA, Kim EK (2012) Triple-negative invasive breast cancer on dynamic contrast-enhanced and diffusion-weighted MR imaging: comparison with other breast cancer subtypes. Eur Radiol 22:1724–1734. https://doi.org/10.1007/s00330-012-2425-2

9. Dietzel M, Baltzer PA, Vag T et al (2011) Potential of MR mammography to predict tumor grading of invasive breast cancer. Rofo 183:826–833. https://doi.org/10.1055/s-0031-1273244
10. Baltzer PA, Vag T, Dietzel M et al (2010) Computer-aided interpretation of dynamic magnetic resonance imaging reflects histopathology of invasive breast cancer. Eur Radiol 20:1563–1571. https://doi.org/10.1007/s00330-010-1722-x
11. Dietzel M, Zoubi R, Vag T et al (2013) Association between survival in patients with primary invasive breast cancer and computer aided MRI. J Magn Reson Imaging 37:146–155. https://doi.org/10.1002/jmri.23812
12. Schipper RJ, van Roozendaal LM, de Vries B et al (2013) Axillary ultrasound for preoperative nodal staging in breast cancer patients: is it of added value? Breast 22:1108–1113. https://doi.org/10.1016/j.breast.2013.09.002
13. van Nijnatten TJA, Ploumen EH, Schipper RJ et al (2016) Routine use of standard breast MRI compared to axillary ultrasound for differentiating between no, limited and advanced axillary nodal disease in newly diagnosed breast cancer patients. Eur J Radiol 85:2288–2294. https://doi.org/10.1016/j.ejrad.2016.10.030
14. Baltzer PA, Dietzel M, Burmeister HP et al (2011) Application of MR mammography beyond local staging: is there a potential to accurately assess axillary lymph nodes? Evaluation of an extended protocol in an initial prospective study. AJR Am J Roentgenol 196: W641–W647. https://doi.org/10.2214/AJR.10.4889
15. Glunde K, Penet MF, Jiang L, Jacobs MA, Bhujwalla ZM (2015) Choline metabolism-based molecular diagnosis of cancer: an update. Expert Rev Mol Diagn 15:735–747. https://doi.org/10.1586/14737159.2015.1039515
16. Baltzer PA, Dietzel M (2013) Breast lesions: diagnosis by using proton MR spectroscopy at 1.5 and 3.0 T–systematic review and meta-analysis. Radiology 267:735–746. https://doi.org/10.1148/radiol.13121856
17. Rageth CJ, O'Flynn EAM, Pinker K et al (2018) Second International Consensus Conference on lesions of uncertain malignant potential in the breast (B3 lesions). Breast Cancer Res Treat. https://doi.org/10.1007/s10549-018-05071-1
18. Bennani-Baiti B, Bennani-Baiti N, Baltzer PA (2016) Diagnostic performance of breast magnetic resonance imaging in non-calcified equivocal breast findings: results from a systematic review and meta-analysis. PLoS One 11:e0160346. https://doi.org/10.1371/journal.pone.0160346
19. Vanhamme L, van den Boogaart A, Van Huffel S (1997) Improved method for accurate and efficient quantification of MRS data with use of prior knowledge. J Magn Reson 129:35–43
20. Haddadin IS, McIntosh A, Meisamy S et al (2009) Metabolite quantification and high-field MRS in breast cancer. NMR Biomed 22:65–76. https://doi.org/10.1002/nbm.1217
21. Baik HM, Su MY, Yu H, Mehta R, Nalcioglu O (2006) Quantification of choline-containing compounds in malignant breast tumors by 1H MR spectroscopy using water as an internal reference at 1.5 T. MAGMA 19:96–104. https://doi.org/10.1007/s10334-006-0032-4
22. Woitek R, Spick C, Schernthaner M et al (2017) A simple classification system (the tree flowchart) for breast MRI can reduce the number of unnecessary biopsies in MRI-only lesions. Eur Radiol 27:3799–3809. https://doi.org/10.1007/s00330-017-4755-6
23. Spick C, Pinker-Domenig K, Rudas M, Helbich TH, Baltzer PA (2014) MRI-only lesions: application of diffusion-weighted imaging obviates unnecessary MR-guided breast biopsies. Eur Radiol 24:1204–1210. https://doi.org/10.1007/s00330-014-3153-6
24. Houssami N, Ciatto S, Macaskill P et al (2008) Accuracy and surgical impact of magnetic resonance imaging in breast cancer staging: systematic review and meta-analysis in detection of multifocal and multicentric cancer. J Clin Oncol 26:3248–3258. https://doi.org/10.1200/JCO.2007.15.2108
25. Clauser P, Mann R, Athanasiou A et al (2018) A survey by the European Society of Breast Imaging on the utilisation of breast MRI in clinical practice. Eur Radiol 28:1909–1918. https://doi.org/10.1007/s00330-017-5121-4
26. Wright GP, Mater ME, Sobel HL et al (2015) Measuring the impact of the American College of Surgeons Oncology Group Z0011 trial on breast cancer surgery in a community health system. Am J Surg 209:240–245. https://doi.org/10.1016/j.amjsurg.2014.07.001
27. Lim GH, Upadhyaya VS, Acosta HA, Lim JMA, Allen JC Jr, Leong LCH (2018) Preoperative predictors of high and low axillary nodal burden in Z0011 eligible breast cancer patients with a positive lymph node needle biopsy result. Eur J Surg Oncol 44:945–950. https://doi.org/10.1016/j.ejso.2018.04.003
28. Harris CK, Tran HT, Lee K et al (2017) Positive ultrasound-guided lymph node needle biopsy in breast cancer may not mandate axillary lymph node dissection. Ann Surg Oncol 24:3004–3010. https://doi.org/10.1245/s10434-017-5935-y
29. Thakur SB, Brennan SB, Ishill NM et al (2011) Diagnostic usefulness of water-to-fat ratio and choline concentration in malignant and benign breast lesions and normal breast parenchyma: an in vivo (1) H MRS study. J Magn Reson Imaging 33:855–863. https://doi.org/10.1002/jmri.22493
30. Suppiah S, Rahmat K, Mohd-Shah MN et al (2013) Improved diagnostic accuracy in differentiating malignant and benign lesions using single-voxel proton MRS of the breast at 3 T MRI. Clin Radiol 68:e502–e510. https://doi.org/10.1016/j.crad.2013.04.002
31. Baek H-M (2012) Diagnostic value of breast proton magnetic resonance spectroscopy at 1.5T in different histopathological types. ScientificWorldJournal 2012:508295. https://doi.org/10.1100/2012/508295
32. Sah RG, Sharma U, Parshad R, Seenu V, Mathur SR, Jagannathan NR (2011) Association of estrogen receptor, progesterone receptor, and human epidermal growth factor receptor 2 status with total choline concentration and tumor volume in breast cancer patients: an MRI and in vivo proton MRS study. Magn Reson Med. https://doi.org/10.1002/mrm.24117
33. Dorrius MD, Pijnappel RM, van der Weide Jansen MC et al (2012) The added value of quantitative multi-voxel MR spectroscopy in breast magnetic resonance imaging. Eur Radiol 22:915–922. https://doi.org/10.1007/s00330-011-2322-0
34. Pinker K, Bogner W, Baltzer P et al (2014) Improved diagnostic accuracy with multiparametric magnetic resonance imaging of the breast using dynamic contrast-enhanced magnetic resonance imaging, diffusion-weighted imaging, and 3-dimensional proton magnetic resonance spectroscopic imaging. Invest Radiol 49:421–430. https://doi.org/10.1097/RLI.0000000000000029
35. Pinker K, Bickel H, Helbich TH et al (2013) Combined contrast-enhanced magnetic resonance and diffusion-weighted imaging reading adapted to the "Breast Imaging Reporting and Data System" for multiparametric 3-T imaging of breast lesions. Eur Radiol 23:1791–1802. https://doi.org/10.1007/s00330-013-2771-8
36. Baltzer A, Dietzel M, Kaiser CG, Baltzer PA (2016) Combined reading of contrast enhanced and diffusion weighted magnetic resonance imaging by using a simple sum score. Eur Radiol 26:884–891. https://doi.org/10.1007/s00330-015-3886-x
37. Baltzer PA, Dietzel M, Kaiser WA (2013) A simple and robust classification tree for differentiation between benign and malignant lesions in MR-mammography. Eur Radiol 23:2051–2060. https://doi.org/10.1007/s00330-013-2804-3
38. Baum F, Fischer U, Vosshenrich R, Grabbe E (2002) Classification of hypervascularized lesions in CE MR imaging of the breast. Eur Radiol 12:1087–1092. https://doi.org/10.1007/s00330-001-1213-1
39. López-Knowles E, Wilkerson PM, Ribas R et al (2015) Integrative analyses identify modulators of response to neoadjuvant aromatase inhibitors in patients with early breast cancer. Breast Cancer Res 17: 35. https://doi.org/10.1186/s13058-015-0532-0

40. Bickel H, Pinker K, Polanec S et al (2017) Diffusion-weighted imaging of breast lesions: region-of-interest placement and different ADC parameters influence apparent diffusion coefficient values. Eur Radiol 27:1883–1892. https://doi.org/10.1007/s00330-016-4564-3
41. Sharma U, Mehta A, Seenu V, Jagannathan NR (2004) Biochemical characterization of metastatic lymph nodes of breast cancer patients by in vitro 1H magnetic resonance spectroscopy: a pilot study. Magn Reson Imaging 22:697–706. https://doi.org/10.1016/j.mri.2004.01.037
42. Dietzel M, Baltzer PA, Dietzel A et al (2010) Application of artificial neural networks for the prediction of lymph node metastases to the ipsilateral axilla - initial experience in 194 patients using magnetic resonance mammography. Acta Radiol Stockh Swed 1987 51:851–858. https://doi.org/10.3109/02841851.2010.498444
43. Lenkinski RE, Wang X, Elian M, Goldberg SN (2009) Interaction of gadolinium-based MR contrast agents with choline: implications for MR spectroscopy (MRS) of the breast. Magn Reson Med 61:1286–1292. https://doi.org/10.1002/mrm.21937
44. Baltzer PA, Gussew A, Dietzel M et al (2012) Effect of contrast agent on the results of in vivo (1) H MRS of breast tumors - is it clinically significant? NMR Biomed 25:67–74. https://doi.org/10.1002/nbm.1714
45. Kuhl CK, Schrading S, Strobel K, Schild HH, Hilgers RD, Bieling HB (2014) Abbreviated breast magnetic resonance imaging (MRI): first postcontrast subtracted images and maximum-intensity projection-a novel approach to breast cancer screening with MRI. J Clin Oncol 32:2304–2310. https://doi.org/10.1200/JCO.2013.52.5386
46. Marshall H, Devine PM, Shanmugaratnam N et al (2010) Evaluation of multicoil breast arrays for parallel imaging. J Magn Reson Imaging 31:328–338. https://doi.org/10.1002/jmri.22023